

GALACTIC COSMIC RAYS FROM PBHs AND PRIMORDIAL SPECTRA WITH A SCALE

Aurélien Barrau, David Blais*, Gaëlle Boudoul, David Polarski*

Institut des Sciences Nucléaires de Grenoble UMR 5821 CNRS-IN2P3,
Université Joseph Fourier, Grenoble-I, France.

* Laboratoire de Physique Mathématique et Théorique, UMR 5825 CNRS,
Université de Montpellier II, 34095 Montpellier, France.

Abstract

We consider the observational constraints from the detection of antiprotons in the Galaxy on the amount of Primordial Black Holes (PBH) produced from primordial power spectra with a bumpy mass variance. Though essentially equivalent at the present time to the constraints from the diffuse γ -ray background, they allow a widely independent approach and they should improve sensibly in the nearby future. We discuss the resulting constraints on inflationary parameters using a Broken Scale Invariance (BSI) model as a concrete example.

PACS Numbers: 04.62.+v, 98.80.Cq

1 Introduction

The formation of PBHs in the early universe is an inevitable prediction based on general relativity, the existence of a hot phase and, most importantly, the presence of primordial fluctuations which are the seed of the large structures in our universe [1]. It can have many interesting cosmological consequences and is one of the few constraints available on the primordial fluctuations on very small scales that can be based on existent astrophysical observations (see e.g. [2]). It has been used by various authors in order to constrain the spectrum of primordial fluctuations, in particular in order to find an upper limit on the spectral index n and on the present relative density of PBHs with $M \approx M_*$ (the initial mass of a PBH whose lifetime equals the age of the Universe) [3],[4],[5]. A possible contribution of evaporating PBHs to the diffuse γ -ray background is presently the most constraining observation [6]. On the other hand, the observation of antiprotons in the Galaxy is as powerful and, in contrast to the γ -ray background, sensitive improvements can be expected in the near future. These involve both experimental and theoretical progress. This is why it is interesting to consider in some details the constraints these observations can, and will, put on any primordial fluctuations model, and prominently on some inflationary models. As noted earlier (see, e.g., Fig.1 in [7]), a constant spectral index n would need extreme fine tuning in order to saturate the γ -ray or antiproton constraint, and such a large n is anyway excluded by the latest CMB data. Hence we consider here spectra with a characteristic scale for which the generation of PBHs is boosted in a certain mass range.

2 PBH formation and primordial fluctuations

Density of PBHs from bumpy mass variance: For detailed confrontation with cosmological and astrophysical observations one often needs the mass spectrum, the number density per unit of mass. This is particularly delicate for PBHs and we follow here a derivation valid in the presence of a bump, as given in [8]. The first assumption is that the primordial spectrum of cosmological fluctuations has a characteristic scale in its power spectrum $P(k)$, which results in a well-localized bump in its mass variance. The importance of this assumption lies in the determination of the PBH mass scale M_{peak} where PBH formation mainly occurs. The second assumption, supported by numerical simulations, is that PBH formation occurs through near-critical collapse [9] whereby PBH with different masses M around $M_{peak} \equiv M_H(t_{k_{peak}})$, the horizon mass at the (horizon-crossing) time $t_{k_{peak}}$ – the horizon crossing time t_k is defined through $k = a(t_k)H(t_k)$ – could be formed at the same time $t_{k_{peak}}$, according to

$$M = \kappa M_H(\delta - \delta_c)^\gamma, \quad (1)$$

where δ_c is a control parameter. While the parameters γ and δ_c are universal with $\gamma \approx 0.35$, $\delta_c \approx 0.7$, the parameter κ (or ϵ , see below) can vary sensibly and

fixes essentially the typical PBH mass. As shown in [8], one finds

$$\frac{d\Omega_{PBH}}{d\ln M} \equiv \frac{d\Omega_{PBH}(M, t_{k_{peak}})}{d\ln M} = \left(\gamma \kappa^{\frac{1}{\gamma}}\right)^{-1} \left(\frac{M}{M_{peak}}\right)^{1+\frac{1}{\gamma}} p[\delta(M)]. \quad (2)$$

If we identify the maximum of (2) in the following way

$$M_{max} = \epsilon M_{peak} , \quad (3)$$

we are led to the result

$$\frac{d\Omega_{PBH}}{d\ln M} = \epsilon^{-\frac{1}{\gamma}} \beta(M_{peak}) \left(1 + \frac{1}{\gamma}\right) \left(\frac{M}{M_{peak}}\right)^{1+\frac{1}{\gamma}} \exp\left[-\epsilon^{-\frac{1}{\gamma}}(1+\gamma) \left(\frac{M}{M_{peak}}\right)^{\frac{1}{\gamma}}\right] , \quad (4)$$

$\beta(M_{peak})$ gives the probability that a region of comoving size $R = (H^{-1}/a)|_{t=t_{k_{peak}}}$ has an averaged density contrast at the time $t_{k_{peak}}$ in the range $\delta_c \leq \delta \leq \delta_{max}$

$$\beta(M_{peak}) = \int_{\delta_c}^{\delta_{max}} p(\delta, t_{k_{peak}}) d\delta . \quad (5)$$

It is then straightforward to find the quantity of interest to us

$$\frac{d^2 n_i}{dM_i dV_i} = \frac{3M_p^2}{32\pi} \left(\frac{M_p}{M_{peak}}\right)^4 x^{-2} \frac{d\Omega_{PBH}}{d\ln M}(x) , \quad (6)$$

where M_p stands for the Planck mass while $x \equiv \frac{M}{M_{peak}}$. The subscript i stands for “initial”, i.e. at the time of formation. The mass M_{peak} corresponds to the maximum in the mass variance $\sigma_H(t_k)$ and *not* to the maximum in the primordial spectrum itself [5]. The parameters γ and ϵ refer to PBH formation while M_{peak} and $\beta(M_{peak})$ refer to the primordial spectrum.

Primordial inflationary fluctuations: One usually considers Gaussian primordial inflationary fluctuations but it should be stressed that non-Gaussianity of the fluctuations could lead to sensibly different results [10]. For primordial fluctuations with a Gaussian probability density $p[\delta]$, we have

$$p(\delta) = \frac{1}{\sqrt{2\pi} \sigma(R)} e^{-\frac{\delta^2}{2\sigma^2(R)}} , \quad \sigma^2(R) = \frac{1}{2\pi^2} \int_0^\infty dk k^2 W_{TH}^2(kR) P(k) , \quad (7)$$

where δ is the density contrast averaged over a sphere of radius R , and $\sigma^2(R) \equiv \left\langle \left(\frac{\delta M}{M}\right)_R^2 \right\rangle$ is computed using a top-hat window function. Usually what is meant by the primordial power spectrum is the power spectrum on superhorizon scales after the end of inflation. On these scales, the scale dependence of the power spectrum is unaffected by cosmic evolution. On subhorizon scales, however, this is no longer the case, and one has instead

$$P(k, t) = \frac{P(0, t)}{P(0, t_i)} P(k, t_i) T^2(k, t) , \quad T(k \rightarrow 0, t) \rightarrow 1 , \quad (8)$$

where t_i is some initial time when all scales are outside the Hubble radius ($k < aH$). Therefore, the power spectrum $P(k)$ on sub-horizon scales appearing in (7) must involve convolution with the transfer function *at time* t_k [7]. At reentrance inside the Hubble radius during the radiation dominated stage, one has *in complete generality* [11],[5] (subscript e stands for the end of inflation)

$$\sigma_H^2(t_k) = \frac{8}{81\pi^2} \int_0^{\frac{k_e}{k}} x^3 F(kx) T^2(kx, t_k) W_{TH}^2(x) dx, \quad t_{k_e} \ll t_k \ll t_{eq}, \quad (9)$$

where the transfer function can be computed analytically and yields

$$T^2(kx, t_k) \equiv \left[\frac{9}{x^2} \left(\frac{\sin(c_s x)}{c_s x} - \cos(c_s x) \right) \right]^2 = W_{TH}^2(c_s x) = W_{TH}^2\left(\frac{x}{\sqrt{3}}\right), \quad (10)$$

while $F(k) \equiv \frac{81}{16} k^3 P(k, t_k) = \frac{81}{8} \pi^2 \delta_H^2(k, t_k)$. Finally $\beta(M_{peak})$ is given by

$$\beta(M_{peak}) \approx \frac{\sigma_H(t_{k_{peak}})}{\sqrt{2\pi} \delta_c} e^{-\frac{\delta_c^2}{2\sigma_H^2(t_{k_{peak}})}}, \quad (11)$$

with $\sigma_H^2(t_{k_{peak}}) \equiv \sigma^2(R)|_{t_{k_{peak}}} \equiv \sigma^2(M_{peak})$, and we will take $\delta_c = 0.7$.

For a given primordial fluctuations spectrum of inflationary origin normalized at large scales using the COBE data, the quantities M_{peak} and $\beta(M_{peak})$ can be computed numerically and will depend on some inflationary parameters specifying that model as well as on cosmological parameters pertaining to the cosmological background evolution [11]. On the other hand γ and ϵ should be found by numerical simulations of PBH formation for this particular spectrum. Values $\epsilon = 0.5, 1, 2$, correspond to $\kappa \approx 2.7, 5.4, 10.8$.

3 Evaporation, fragmentation and source term

As shown by Hawking [12], such PBHs should evaporate into particles of energy Q per unit of time t (for each degree of freedom):

$$\frac{d^2 N}{dQ dt} = \frac{\Gamma_s}{h \left(\exp\left(\frac{Q}{h\kappa/4\pi^2 c}\right) - (-1)^{2s} \right)}, \quad (12)$$

where contributions of angular velocity and electric potential have been neglected since the black hole discharges and finishes its rotation much faster than it evaporates [13]. The quantity κ is the surface gravity, s is the spin of the emitted species and Γ_s is the absorption probability. If the Hawking temperature, defined by $T = hc^3/(16\pi kGM) \approx (10^{13} \text{g}/M) \text{ GeV}$ is introduced, the argument of the exponent becomes simply a function of Q/kT . Although the absorption probability is often approximated by its relativistic limit, we took into account in this work its real expression for non-relativistic particles:

$$\Gamma_s = \frac{4\pi\sigma_s(Q, M, \mu)}{h^2 c^2} (Q^2 - \mu^2), \quad (13)$$

where σ_s is the absorption cross section computed numerically [14] and μ is the rest mass of the emitted particle.

Among other cosmic rays emitted by evaporating PBHs, antiprotons are especially interesting as their secondary flux is both rather small (the \bar{p}/p ratio near the Earth is lower than 10^{-4} at all energies) and quite well known [18]. We will therefore focus on such antiparticles in this paper. As shown by MacGibbon and Webber [15], when the black hole temperature is greater than the quantum chromodynamics confinement scale Λ_{QCD} , quarks and gluons jets are emitted instead of composite hadrons. To evaluate the number of emitted antiprotons \bar{p} , one therefore needs to perform the following convolution:

$$\frac{d^2 N_{\bar{p}}}{dE dt} = \sum_j \int_{Q=E}^{\infty} \alpha_j \frac{\Gamma_{s_j}(Q, T)}{h} \left(e^{\frac{Q}{kT}} - (-1)^{2s_j} \right)^{-1} \times \frac{dg_{j\bar{p}}(Q, E)}{dE} dQ, \quad (14)$$

where α_j is the number of degrees of freedom, E is the antiproton energy and $dg_{j\bar{p}}(Q, E)/dE$ is the normalized differential fragmentation function, *i.e.* the number of antiprotons between E and $E + dE$ created by a parton jet of type j and energy Q . The fragmentation functions have been evaluated with the high-energy physics event generator PYTHIA/JETSET [16] based on the string fragmentation model.

Once the spectrum of emitted antiprotons is known for a single PBH of given mass, the source term used for propagation can be obtained through

$$\frac{d^3 N_{\bar{p}}^{\odot}}{dE dt dV}(E) = \int_0^{\infty} \frac{d^2 N_{\bar{p}}}{dE dt}(M, t_0) \frac{d^2 n}{dM dV_i} dM \left(\frac{a(t_0)}{a(t_{form})} \right)^{-3} \frac{\rho_{\odot}}{\langle \rho_M \rangle}, \quad (15)$$

where $d^2 n/dM dV_i$ is the mass spectrum modified by Hawking evaporation until today, $a(t_0)$ and $a(t_{form})$ are the scale factors of the Universe nowadays and at the formation time t_{form} (which is a function of the PBH mass), ρ_{\odot} is the local halo density and $\langle \rho_M \rangle$ is the mean matter density in the present Universe. The dilution factor, for $t_{form} \ll t_{eq}$, applies to all universes of interest. The last term converts the mean density into the local density under the reasonable assumption that the clustering of PBHs follows the main dark matter component. The quantity $d^2 n/dM dV_i$ can be obtained through the mass loss rate which reads $dM/dt = -\alpha(M)/M^2$ (by simple integration of the Hawking spectrum multiplied by the energy of the emitted quantum) where $\alpha(M)$ accounts for the available degrees of freedom at a given mass. With the assumption $\alpha(M) \approx \text{const}$ it leads to:

$$\frac{d^2 n}{dM dV_i}(M) = \frac{M^2}{(3\alpha t + M^3)^{2/3}} \cdot \frac{d^2 n_i}{dM_i dV_i}((3\alpha t + M^3)^{1/3}). \quad (16)$$

Hence the spectrum nowadays is essentially identical to the initial one above $M_* \equiv 3\alpha t_0 \approx 5 \times 10^{14} \text{g}$ and proportional to M^2 below.

4 Propagation and source distribution

The propagation of the antiprotons produced by PBHs in the Galaxy has been studied in the two zone diffusion model described in [17] & [18]. In this model, the geometry of the Milky-Way is a cylindrical box whose radial extension is $R = 20$ kpc from the galactic center, with a disk whose thickness is $2h = 200$ pc and a diffusion halo whose extension is still subject to large uncertainties.

The five parameters used in this model are: K_0 , δ (describing the diffusion coefficient $K(E) = K_0 \beta R^\delta$), the halo half height L , the convective velocity V_c and the Alfvén velocity V_a . They have been varied within a given range determined by an exhaustive and systematic study of cosmic ray nuclei data [17] and chosen at their mean value. The same parameters used to study the antiproton flux from a scale-free unnormalised power spectrum in [19] are used again in this analysis. The antiproton spectrum is affected by energy losses when \bar{p} interact with the galactic interstellar matter and by energy gains when reacceleration occurs. These energy changes are described by an intricate integro-differential equation [19] where a source term $q_i^{ter}(E)$ was added, leading to the so-called tertiary component which corresponds to inelastic but non-annihilating reactions of \bar{p} on interstellar matter. Performing Bessel transforms, all the quantities can be expanded over the orthogonal set of Bessel functions of zeroth order and the solution of the equation for antiprotons can be explicitly obtained [17].

The spatial distribution of PBHs (normalized to the local density) was assumed to follow a usual spherically symmetric isothermal profile where the core radius R_c has been fixed to 3.5 kpc and the centrogalactic distance of the solar system R_\odot to 8 kpc. Uncertainties on R_c and the consequences of a possible flatness have been shown to be irrelevant in [19]. The dark halo extends far beyond the diffusion halo whereas its core is grossly embedded within L . The sources located inside the dark matter halo but outside the magnetic halo were shown to have a negligible contribution.

5 Experimental data and inflationary models

The astrophysical parameters describing the propagation within the galaxy being determined, for each set of initial parameters $(\beta(M_{peak}), M_{peak}, \epsilon, \gamma)$ defining the mass spectrum given in section 1, a \bar{p} -spectrum is computed. Fig. 1 gives the experimental data together with theoretical spectra for $\beta(M_{peak}) = 5 \times 10^{-28}$ and $\beta(M_{peak}) = 10^{-26}$ while $M_{peak} = M_*$, $\epsilon = 1$ and $\gamma = 0.35$. The first curve is in agreement with data whereas the second one clearly contradicts experimental results and excludes such a PBH density. It should be emphasized that the computed spectra are not only due to primary antiprotons coming from PBHs evaporation but also to secondary antiprotons resulting from the spallation of cosmic rays on the interstellar matter. The method used to accurately take into account such secondaries is described in [18] and relies on a very detailed treat-

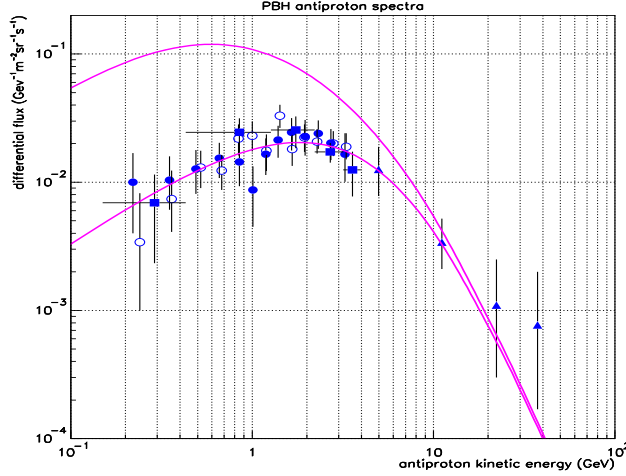


Figure 1: Experimental data from BESS95 (filled circles), BESS98 (circles), CAPRICE (triangles) and AMS (squares) superimposed with PBH and secondary spectra for $\beta(M_{peak}) = 5 \times 10^{-28}$ (lower curve) and $\beta(M_{peak}) = 10^{-26}$ (upper curves). In both cases, $M_{peak} = M_*$, $\epsilon = 1$ and $\gamma = 0.35$.

ment of proton-nuclei and nuclei-nuclei interactions near threshold thanks to a fully partonic Monte-Carlo program. The uncertainties associated with the theoretical description of cosmic-rays diffusion in the Galaxy (coming from degeneracy of the model with respect to several parameters, from nuclear cross sections and from a lack of measurements of some astrophysical quantities) are described in [18] & [19] and are taken into account in this work. To derive a reliable upper limit, and to account for asymmetric error bars in data, we define a generalized χ^2 as

$$\chi^2 = \sum_i \frac{(\Phi^{th}(Q_i) - \Phi_i^{exp})^2}{(\sigma_i^{exp+} + \sigma^{th+}(Q_i))^2} \Theta(\Phi^{th}(Q_i) - \Phi_i^{exp}) + \sum_i \frac{(\Phi^{th}(Q_i) - \Phi_i^{exp})^2}{(\sigma_i^{exp-} + \sigma^{th-}(Q_i))^2} \Theta(\Phi_i^{exp} - \Phi^{th}(Q_i)), \quad (17)$$

where σ^{th+} and σ^{exp+} (σ^{th-} and σ^{exp-}) are the theoretical and experimental positive (negative) uncertainties, $\Phi^{th}(Q_i)$ and Φ_i^{exp} are the theoretical and experimental antiproton fluxes at energy Q_i . Requiring this χ^2 to remain small enough, a statistically significant upper limit is obtained.

The maximum allowed values of $\beta(M_{peak})$ obtained by this method are displayed in Fig. 2 as a function of M_{peak} for $\epsilon = 0.5, 1, 2$ with $\gamma = 0.35$. As expected, the most stringent limit is obtained when $M_{max} = M_*$ (*i.e.* $\epsilon M_{peak} = M_*$). The curve is clearly asymmetric because the mass spectrum is exponentially suppressed at M_* when $M_{peak} < M_*$ whereas it decreases as a power law when $M_{peak} > M_*$. This constraint is significantly stronger than the gravitational one,

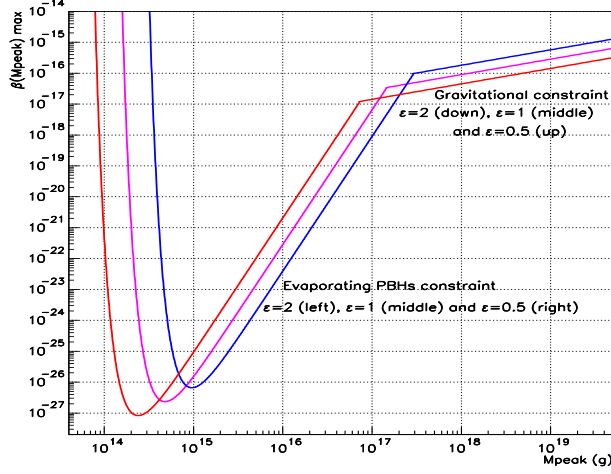


Figure 2: Maximum allowed value $\beta(M_{peak})$ as a function of M_{peak} with $\gamma = 0.35$ and $\epsilon = 0.5, 1, 2$. The gravitational constraint is computed consistently assuming critical collapse from a bumpy mass variance at all scales. The antiproton constraint is significantly stronger than the gravitational constraint in the region $M_* \lesssim M_s \lesssim 100M_*$.

the requirement $\Omega_{PBH,0} < \Omega_{m,0}$, displayed on the right hand side of the plot. In order to constrain inflationary models producing a bump in the mass variance, one has to compute the values M_{peak} and $\beta(M_{peak})$. These will depend on the parameters of the inflationary model considered and can be usually traced back to the microscopic lagrangian. A numerical computation of $\beta(M)$ must be performed for each model using spectra normalized on large scales with the COBE (CMB) data for given cosmological background parameters, e.g. $\Omega_{\Lambda,0} = 1 - \Omega_{m,0}$ [11]. In particular, in a flat universe with $\Omega_{\Lambda,0} = 0.7$, the mass variance at the PBH formation time is reduced by about 15% compared to a flat universe with $\Omega_{m,0} = 1$.

To illustrate how inflationary models can be constrained, we use here a so-called BSI model [20] for which the quantities M_{peak} and $\beta(M_{peak})$ can be found numerically using the analytical expression for its primordial power spectrum. The quantity $F(k)$ is fixed by two inflationary parameters p and k_s and exhibits a jump with large oscillations in the vicinity of k_s , and the relative power between large and small scales is given by p^2 (an analytical expression for $F(k)$ and relevant figures can be found in [20],[5]). This feature derives from a jump in the first derivative of the inflaton potential at the scale k_s so that one of the slow-roll conditions is broken and the resulting spectrum is quite universal [20]. Using the formalism of Section 1 one finds k_{peak} , which must be distinguished from k_s , as well as $\beta(M_{peak})$. Numerical calculations give $M_s \equiv M(t_{k_s}) \approx 1.6 M_{peak}$. We are interested in spectra with $p < 1$, corresponding to more power on small scales. In

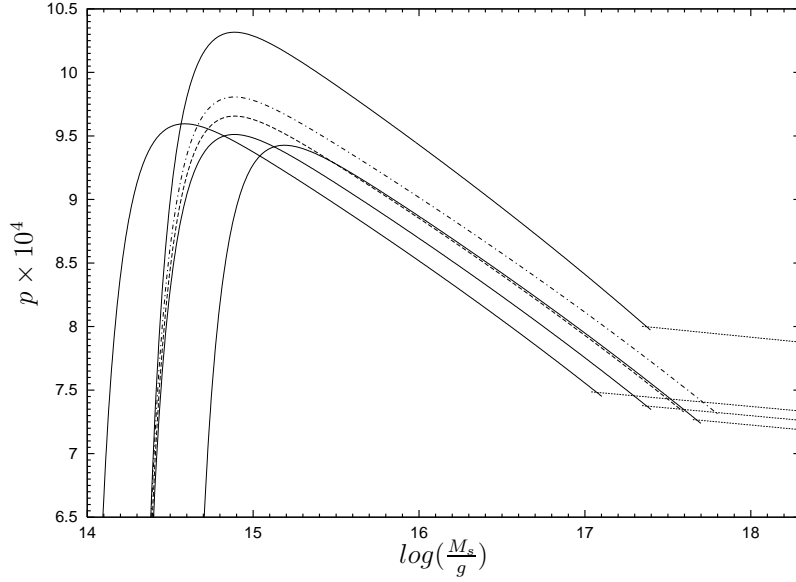


Figure 3: The minimal value of the inflationary parameter p is shown in function of $M_s \equiv M_H(t_{k_s})$ together with the gravitational constraint (straight lines). For given values $(\epsilon, \Omega_{\Lambda,0})$, the region *under* the corresponding curve is excluded by observations. The three solid curves at the bottom ($\epsilon = 2, 1, 0.5$, from the left to the right) are the current constraints for $\Omega_{\Lambda,0} = 0.7$, the upper solid curve corresponds to $\Omega_{m,0} = 1$ and $\epsilon = 1$. The two dashed curves, both for $(1, 0.7)$ show the improvement expected if no antideuteron will be found (the lower, resp. upper curve refers to AMS, resp. GAPS).

Fig. 3, the constraint on the inflationary parameter p is displayed as a function of M_s . In other words each point in the plane $M_{peak}, \beta(M_{peak})$ is translated into the corresponding point k_s, p . As p decreases, the bump in $\sigma_H(t_k)$ and $\beta(M)$ increases. The constant spectral index n (already excluded by recent CMB data) which would pass successfully the antiproton constraint corresponds to $n \approx 1.32$, only slightly less than $n=1.33$, the value satisfying the gravitational constraint at $M_s \simeq M_*$ [5]. Indeed, as mentioned in the Introduction, a small change in n gives a large variation in $\beta(M_*)$.

6 Discussion

Several improvements of our work can be expected in the forthcoming years. On the theoretical side, a better understanding of possible QCD halos appearing near the event horizon of PBHs should slightly alter the expected antiprotons fluxes. The very same computation should also be performed for gamma-rays, following, *e.g.* [6], and compared to the previously obtained limit on β in [3] and [8]. Although essentially independent, the results are expected to be close to the ones obtained here.

On the experimental side, the AMS experiment [21] should provide extremely accurate data of the antiproton flux on a very wide energy range. It should also be sensitive to low energy antideuterons which could substantially improve the current upper limit on the PBH density. According to [22], if no antideuteron is found in three years of data, the limit on $\beta(M_{peak})$ will be improved by a factor of 6. Furthermore, the GAPS project [23], if actually operated in the future, would improve the bound by a factor of 40.

References

- [1] Ya. B. Zeldovich, I. D. Novikov, Sov. Astron. 10 (1967) 602;
B. J. Carr, S. W. Hawking, Mon. Not. R. Astr. Soc. 168 (1974) 399;
B. J. Carr, Astrophys. J. 205 (1975) 1.
- [2] I. D. Novikov, A. G. Polnarev, A. A. Starobinsky, Ya. B. Zeldovich, Astronomy and Astrophysics 80 (1979) 104;
B. J. Carr, in *Observational and theoretical aspects of relativistic astrophysics and cosmology* (1985) edited by J.L. Sanz and L.J. Goicoechea (World Scientific, Singapore).
- [3] B. J. Carr, J. E. Lidsey, Phys. Rev. D 48 (1993) 543;
B. J. Carr, J. H. Gilbert, J. E. Lidsey, Phys. Rev. D 50 (1994) 4853.
- [4] A. M. Green, A. R. Liddle, Phys. Rev. D 56 (1997) 6166.
- [5] D. Blais, T. Bringmann, C. Kiefer, and D. Polarski, astro-ph/0206262;
D. Blais, C. Kiefer, D. Polarski, Phys. Lett. B 535 (2002) 11.
- [6] J. H. MacGibbon, B. J. Carr, Phys. Rept. 307 (1998) 141.
- [7] T. Bringmann, C. Kiefer, and D. Polarski, Phys. Rev. D 65 (2002) 024008.
- [8] J. Yokoyama, Phys. Rev. D 58 (1998) 107502.
- [9] J.C. Niemeyer and K. Jedamzik, Phys. Rev. Lett. 80 (1998) 5481;
J.C. Niemeyer and K. Jedamzik, Phys. Rev. D 59 (1999) 124013.
- [10] J.S. Bullock and J. R. Primack, Phys. Rev. D 55 (1997) 7423.
- [11] D. Polarski, Phys. Lett. B 528 (2002) 193
- [12] S.W. Hawking, Comm. Math. Phys. 43 (1975) 199.
- [13] G.W. Gibbons, Comm. Math. Phys. 44 (1975) 245;
Page D.N., Phys. Rev. D 16 (1977) 2402.
- [14] Page D.N., PhD thesis (1976) Caltech.

- [15] MacGibbon J.H., Webber B.R., Phys. Rev. D 31 (1990) 3052.
- [16] Tjöstrand T., Computer Phys. Commun., 82 (1994) 74.
- [17] D. Maurin, F. Donato, R. Taillet, & P. Salati, ApJ, 555 (2001) 585.
- [18] F. Donato, D. Maurin, P. Salati, A. Barrau, G. Boudoul *et al.*, ApJ 536 (2001) 172-184.
- [19] A. Barrau, G. Boudoul, F. Donato, D. Maurin *et al.*, A&A 388 (2002) 676.
- [20] A. A. Starobinsky, JETP Lett. 55 (1992) 489.
- [21] A. Barrau, Proceedings of the Rencontres de Moriond, Very High Energy Phenomena in the Universe (January 20-27, 2001), astro-ph/0106196.
- [22] A. Barrau, G. Boudoul, F. Donato, D. Maurin, P. Salati *et al.*, astro-ph/0207395.
- [23] K. Mori, C.J. Hailey, E.A. Baltz, W.W. Craig *et al.*, ApJ 566 (2002) 604-616.